

Effect of Stratus on Solar Radiation: A Study Using Millimeter Wave Cloud Radar and Microwave Radiometer Data From the Southern Great Plains

*M. Sengupta and T. P. Ackerman
Pacific Northwest National Laboratory
Richland, Washington*

*E. E. Clothiaux
The Pennsylvania State University
University Park, Pennsylvania*

Introduction

Clouds are important players in the global radiation budget with low-level water clouds being one of the most influential types. Classified as stratocumulus and stratus, these water clouds cover 34% of oceans and 18% of land at any given time (Considine et al. 1997). A 50% plus global coverage, a high albedo when compared to the ocean, and temperatures comparable to the surface causes the low stratiform clouds to provide about 60% of the annually averaged net cloud radiative forcing (Hartmann et al. 1992). Therefore, variations in low cloud cover may have a significant impact on climate change. Additionally, changes in the microphysical properties of stratiform cloud quantified by the liquid water path (LWP) and size distribution may result in changes in albedo. This change in albedo, as a result of changes in microphysics, can impact climate change even if variations in cloud cover do not occur. Our goal is to study variations in the microphysical properties of stratus and their effect on solar radiation, thereby providing an assessment of the comparative importance of the various parameters, defining the warm cloud microphysics. We make use of data from the Southern Great Plains (SGP) Atmospheric Radiation Measurement (ARM) Cloud and Radiation Testbed (CART) site Central Facility (CF) as we require a statistically significant sample size for our study.

Methodology and Theory

The Millimeter Wave Cloud Radar (MMCR), Micropulse Lidar (MPL) and Belfort Ceilometer (BLC) data are used in combination to identify single-layer clouds (Clothiaux 2000). Atmospheric profiles are obtained from a combination of radio-sondes, thermal interferometer, Microwave Radiometer (MWR), surface observations, and National Oceanic and Atmospheric Administration (NOAA) Forecast System Laboratory's Rapid Update Cycle (RUC) model output. The LWP is retrieved from the MWR data (Liljegren 2000). Single-layer water clouds are selected using a temperature threshold for the MMCR derived cloud top and a lognormal drop size distribution is assumed. The familiar relationship defining effective radius (Hansen and Travis 1974)

$$r_{\text{eff}} = \frac{\int r^3 n(r) dr}{\int r^2 n(r) dr} \quad (1)$$

is useful for defining the size parameter of a cloud where $n(r)$ is the representative size distribution (log-normal in our case) and r the physical radius of a water drop assuming sphericity. Using r_{eff} simplifies the expression for optical depth

$$\tau = \frac{3Q_{\text{ext}} \text{LWP}}{4\rho_w r_{\text{eff}}} \quad (2)$$

where Q_{ext} is the extinction efficiency (assumed constant for individual wavelength bands used in our radiative transfer calculation) and ρ_w is the density of water. Using reasonable effective radii values occurring in nature Q_{ext} asymptotes to two for solar wavelengths.

Drop concentrations for a cloud can be calculated using cloud boundaries from the MMCR, MPL, BLC combination, a given effective radius, and a drop-size standard deviation (log-normal width σ_{\log} in our case). Additionally, using Mie theory, for a given radius and width, asymmetry parameters and single-scattering albedos can be calculated for each wavelength band in consideration, assuming constant refractive indices for the individual bands.

As our ultimate interest is in cloud-radiation interactions, we compare observed and modeled solar broadband fluxes for single-layer stratus in order to estimate the performance of size retrievals. A δ -2stream radiative transfer scheme using k distribution and correlated- k technique for spectral integration is used for radiative transfer calculations (Kato et al. 1997). Aerosol optical depths derived from the Multi-filter Rotating Shadowband Radiometer (MFRSR) (Harrison et al. 1994) data are used in our radiative transfer calculations as they have a significant impact in clear-sky cases. A Lundholm curve is fitted to the MFRSR optical depth data, available for five wavelengths, for usage in calculations over 32 spectral bands over the solar spectrum. Ozone optical depths available from the Total Ozone Mapping Spectrometer (TOMS) data aboard the Earth Probe Satellite and wavelength dependent Rayleigh optical depths based on standard profiles (Hansen and Travis 1974) are subtracted before the interpolation. The aerosol absorption calculations assume a composition of mineral dust. Figure 1 delineates our approach to flux calculations.

Cloud Forcing

As downwelling surface solar flux is dependent on solar zenith angle, its effects are removed by normalization as represented by,

$$CF_o(t) = [F_{\text{act},o}(t) - F_{\text{clr},o}(t)]/F_{\text{clr},o}(t) \quad (3)$$

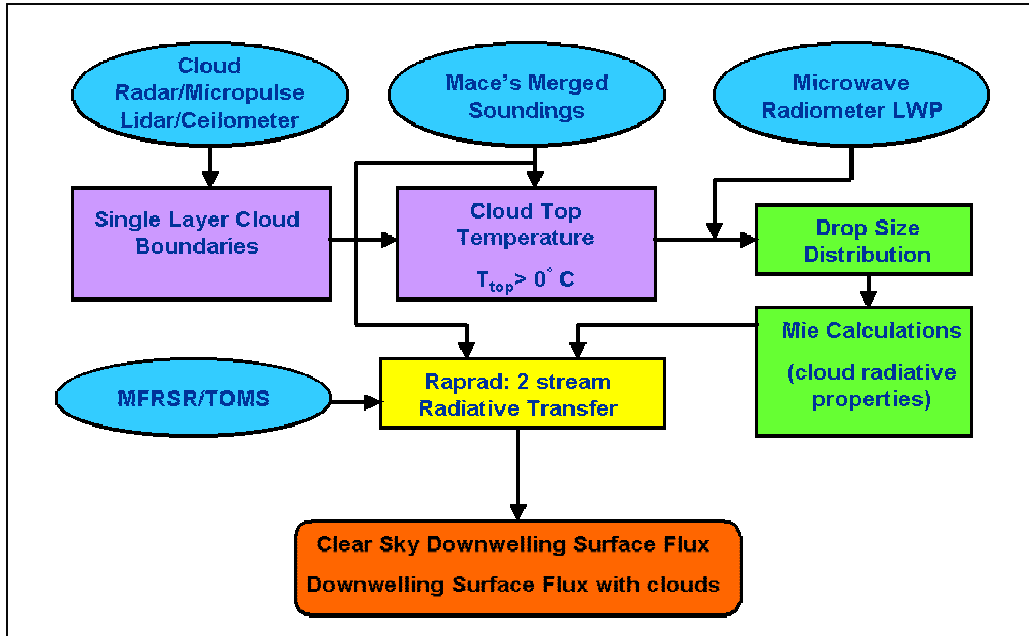


Figure 1. Flowchart illustrating the downwelling flux calculation procedure.

for observations. $CF_o(t)$ is the observed cloud forcing, $F_{act,o}(t)$ the actual downwelling solar flux, and $F_{clr,o}(t)$ the interpolated clear-sky solar flux (Long 1999). For calculations the cloud forcing is,

$$CF_c(t) = f \times [F_{cld,c}(t) - F_{clr,c}(t)] / F_{clr,c}(t) \quad (4)$$

where $F_{cld,c}(t)$ is the calculated flux with clouds, $F_{clr,c}(t)$ is the calculated clear-sky flux, and f the fractional cloud cover over our retrieval domain. The fractional cover is used to weight our calculations for broken cloud cover effects on the domain. Note that f is absent for observations (Eq. 3) as the fractionality is implicit in measurements. The values of $CF(t)$ generally range from -1 to 0 but values greater than 0 are possible due to cloud inhomogeneities. In our study, we ignore cases with observations that have values of cloud forcing greater than 0. Our procedure does not have the capability to reflect these positive values. The physical interpretation of cloud forcing implies that larger negative values and larger magnitudes are analogous to thicker clouds with higher optical depths and reflectivities.

Skill Score Evaluation Technique

In our study, a calculation of downwelling solar flux using a fixed width and effective radius, defined as climatological value, is used as control. A set of effective radii from retrievals using MMCR and MWR data (Kato. et al. 2001) is also used for surface downwelling flux calculations and denoted as best estimate of flux. The observations are from the Basic Radiation System (BRS) suite of instruments located at the CF of the SGP site (Long et al. 1999).

The calculation of a correlation coefficient between the observed, climatological, and best estimate normalized forcing values does not sufficiently represent the nature of variation in the datasets. Therefore, a technique used by the forecasting community is used to resolve the variances in the datasets. A skill score, a quantitative evaluation of the performance of the retrievals, relative to the climatology, with the observations as truth, is calculated. If we define the best estimate results as forecast (F), the climatological results as control (C), and the measured values as observed (O) the mean square error of the forecast (MSE_f), for our calculations, is,

$$MSE_f = \frac{1}{N} \sum (F_i - O_i)^2 \quad (6)$$

where N is the number of data points, and the subscripts denote the individual values of F and O. A mean square error for control can similarly be defined by replacing F with C in (6). Eq. (6) can also be represented in the form,

$$MSE_f = (\bar{F} - \bar{O})^2 + (1 - R_{fo})(S_f^2 - S_o^2) + R_{fo}(S_f - S_o)^2 \quad (7)$$

where the overbars represent the respective means, S's with subscripts represents the standard deviations. R_{fo} represents the correlation coefficient of the forecast and observed datasets. The three terms in Eq. (7) represent the bias error squared (B_f), the non-systematic errors (N_f) and the variance error (V_f), respectively. These three terms provide an insight into the errors in the forecast or control datasets when compared to observations. The skill score (SS) of the forecast is,

$$SS = 1 - MSE_f / MSE_c \quad (8)$$

where the subscripts identify the datasets. A value of 0 shows no skill while positive values show better forecasting skill. The SS and MSE values are used in our analysis of the normalized cloud forcing data and are presented next.

We use 35 days of data for the time period between January 1997 and January 1998 and use a 1-minute resolution for our broadband calculations.

Results

The use of plane-parallel clouds is a good approximation when we have cloud fractions close to 1 or when the sky is overcast. Nevertheless, we use normalized cloud forcing, weighted by the cloud fraction to account for cases for which the cloud fraction is not unity. To obtain a cloud fraction we use the MMCR, MPL, BLC combination and take the fraction of positive cloud detections in the total number of measurements during each calculation period. In our case the data is at 10 seconds resolution while our calculation is done for a 60-second averaging period. We therefore have 6 measurements per calculation period from which we derive our cloud fraction. This cloud fraction is based on the assumption that spatial and temporal averaging is identical. Note that we have selected days with stratus and therefore, have mostly overcast cases. It is interesting that in many cases the LWP values for stratus

lie close to the noise floor of the MWR, leading to uncertainties in the LWP that may even be around 100% (Figure 2). This uncertainty in LWP translates directly to comparable levels of uncertainty in the calculation of cloud optical depth.

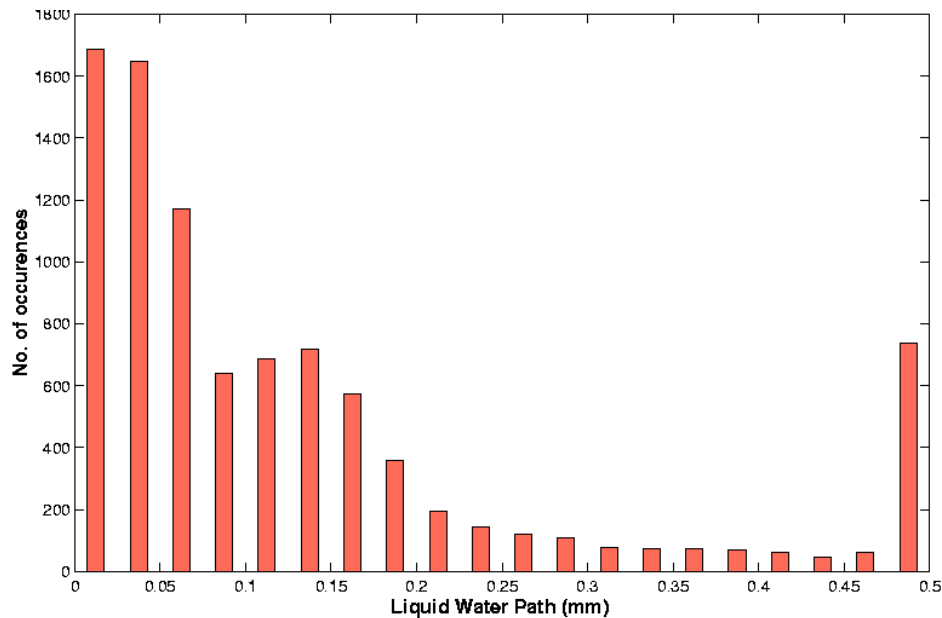


Figure 2. Histogram showing 1 minute averaged LWP from 20-second data (9261 points in 0.025 mm bins) for daytime stratus case occurring between January 1997 and January 1998. Note that negative liquid water values occurring due to instrument noise have been replaced by interpolation using neighboring positive values if there is positive stratus detection using the MMCR, BLC, MPL combination. All points above 0.475 mm are shown as the last bar in the histogram for convenience.

The distribution of retrieved effective radii for our daytime cases (using the Kato et. al 2000 technique) is approximately gaussian (Figure 3) with a median value of 6.61 μm . The effective radius is assumed constant for a profile and retrieved values over 15 μm are not considered. The climatological effective radius is taken to be 7.5 μm . This value is used as it minimizes the net bias in calculated normalized cloud forcing when compared with corresponding observations. The scatter in retrieved normalized forcing (Figure 4b) is higher than the scatter in the forcing calculations using climatological radius (Figure 4a) when both are compared to a common set of observations. The correlation coefficient of control to observation R_{c_0} is 0.76, while the correlation of forecast to observation R_{f_0} is 0.66. Therefore, there is significant correlation in both cases with the fixed radius calculations showing a better correlation to the observations than the retrievals. Table 1 shows the mean square errors divided into components for both the control and the forecast when compared with the observed forcing values. The mean square error for the control is seen to be nearly 40% less than that of forecast. The main source of error is seen to be the bias in the forecast although the random error is also significantly less in the control. Overall, the performance of the climatological effective radius is seen to be better than that of the retrievals. This is also obvious as the skill score SS is -0.41 , a negative value, which shows no skill as far as the retrievals are concerned.

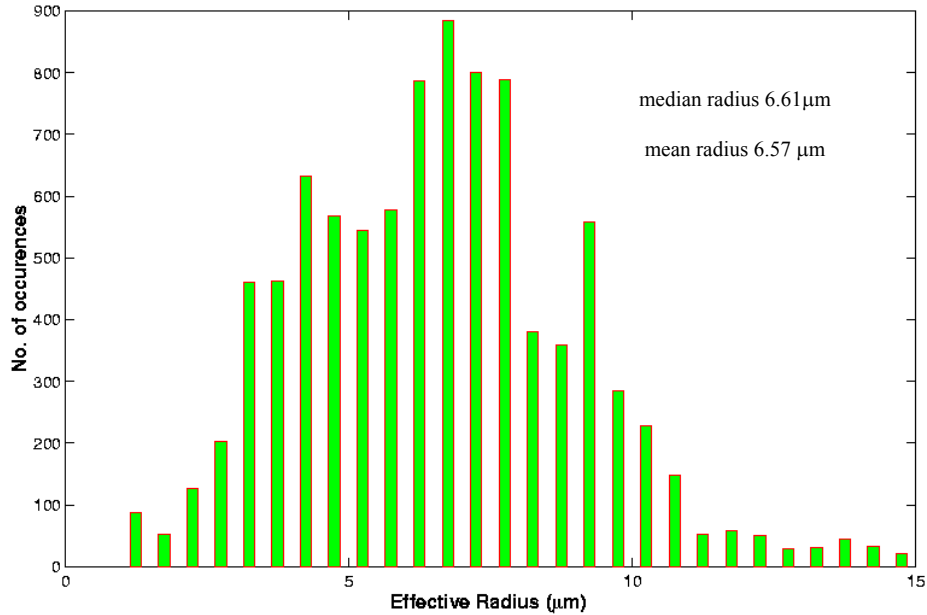


Figure 3. Effective radii (9216 points in 0.5 μm bins) from the MMCR, MWR, and LWP retrievals. The values used in this distribution are from the same times as those used for daytime stratus calculations. The median radius is 6.61 μm and the mean is 6.57 μm .

Table 1. Components of the Mean Square Error of Control and Forecast When Compared to Observations

	Bias²	Random	Variance	Total
MSE _{co}	0.000094	0.027237	0.000997	0.028329
MSE _{fo}	0.001317	0.038013	0.001052	0.040382

The regression coefficients for the least squares shows that most of the bias arises due to higher cloud forcing values when the observed forcings are low (solid black line in Figures 4a and 4b). This may be the result of an overestimate in liquid water, an underestimate of the effective radius or the result of using a plane parallel cloud when we have a broken cloud cover in reality. Another possibility is the absence of sensitivity of LWP retrievals at lower values due to uncertainties in the measured brightness temperatures. A histogram of cloud forcing (Figure. 6) shows that most of the cloud forcings have values less than -0.4 and the median of the observed normalized forcings is seen to be -0.65 . Thus, the smaller end of the forcing scale produces a disproportionate effect on the zeroth order coefficient of the regression.

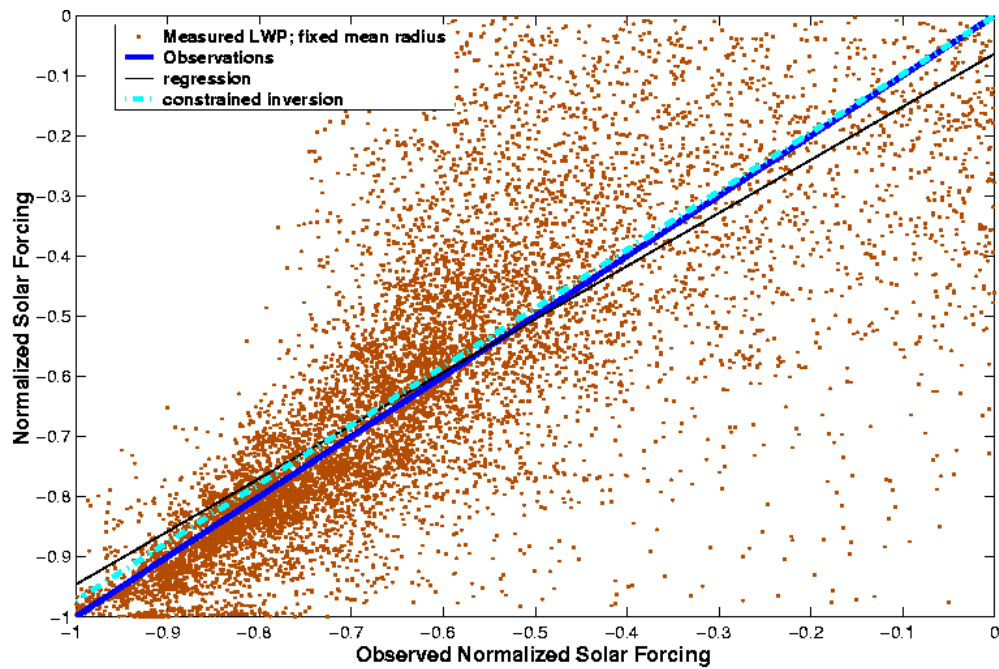


Figure 4a. Scatter plot of the normalized forcing using fixed effective radius of 7.5 μm (control). The regression coefficients are listed in Table 2.

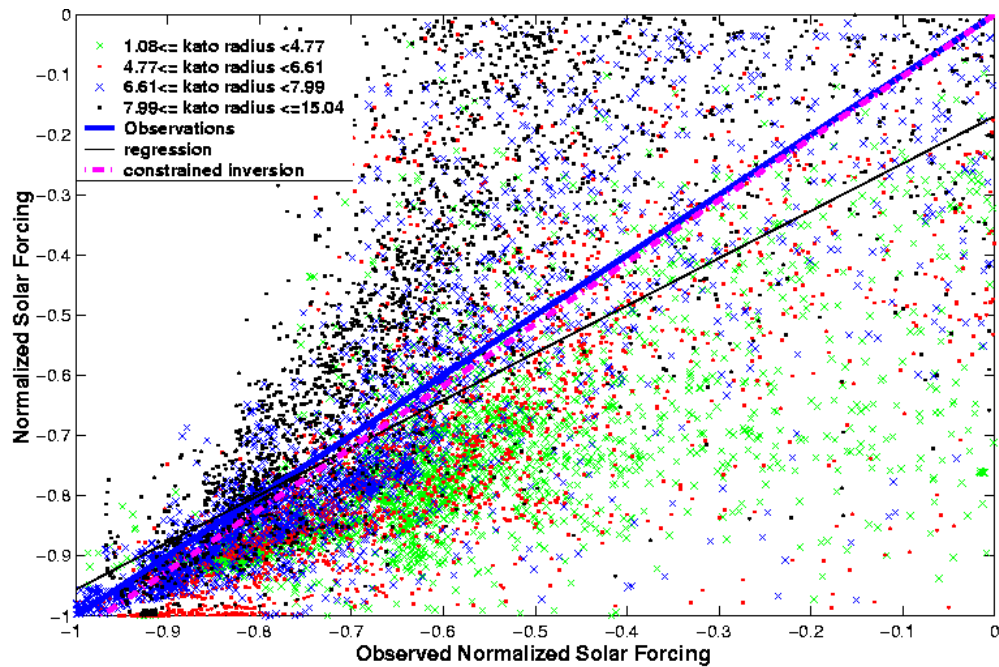


Figure 4b. Scatter plot of the normalized forcing using retrieved radii (forecast). The forecast points are shown in different colors to represent the radii divided into quartiles. The regression coefficients are listed in Table 2.

Table 2. Regression coefficients for the least squares fit to the normalized cloud forcing data. The correlation coefficients are also shown. The black solid and pink dotted lines in Figures 5a and 5b are the fits using the coefficients in this table.

Least Squares Fit	Correlation Coefficient R	Regression Coefficients (unconstrained)	Regression Coefficient (constrained) $a_0=0$
Control to Observations	$R_{co} = 0.76$	$a_0 = -0.063$	$a_1 = 0.973$
		$a_1 = 0.883$	
Forecast to Observations	$R_{fo} = 0.67$	$a_0 = -0.169$	$a_1 = 1.029$
		$a_1 = 0.787$	

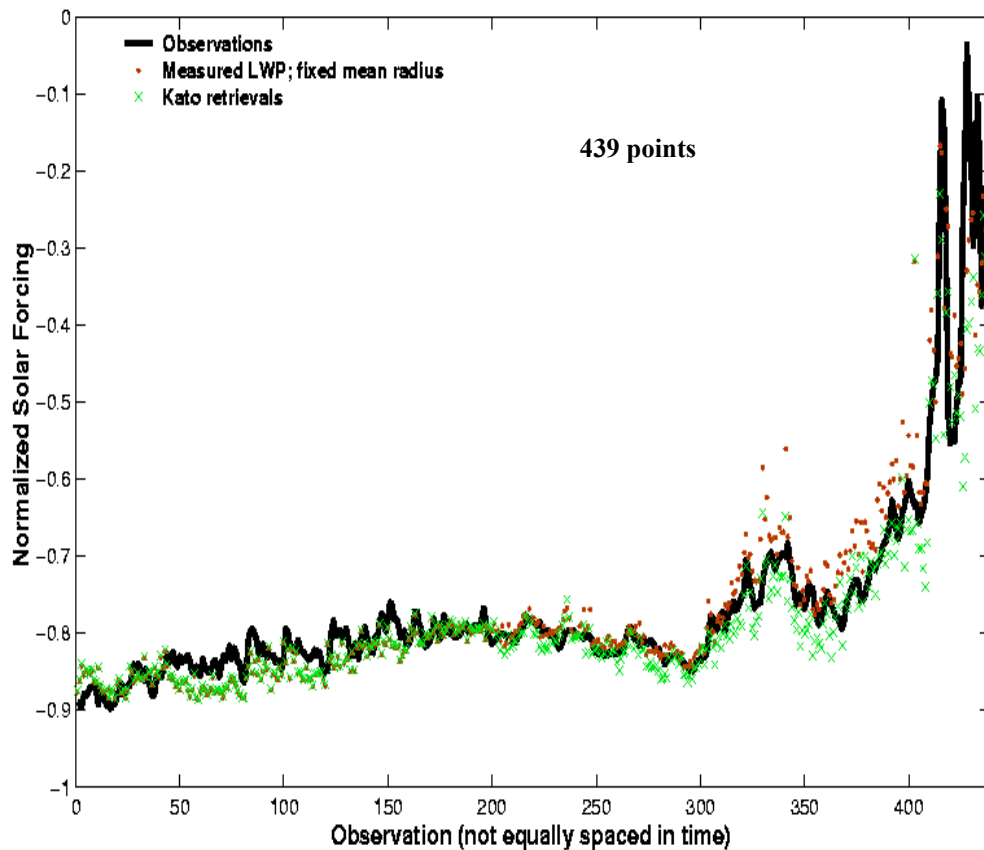


Figure 5a. Time series of normalized forcing (1 minute averaged calculations) for January 1, 1997. The rms error for the climatological radius of $7.5 \mu\text{m}$ is 0.051, while it is $0.058 \mu\text{m}$ for the retrievals.

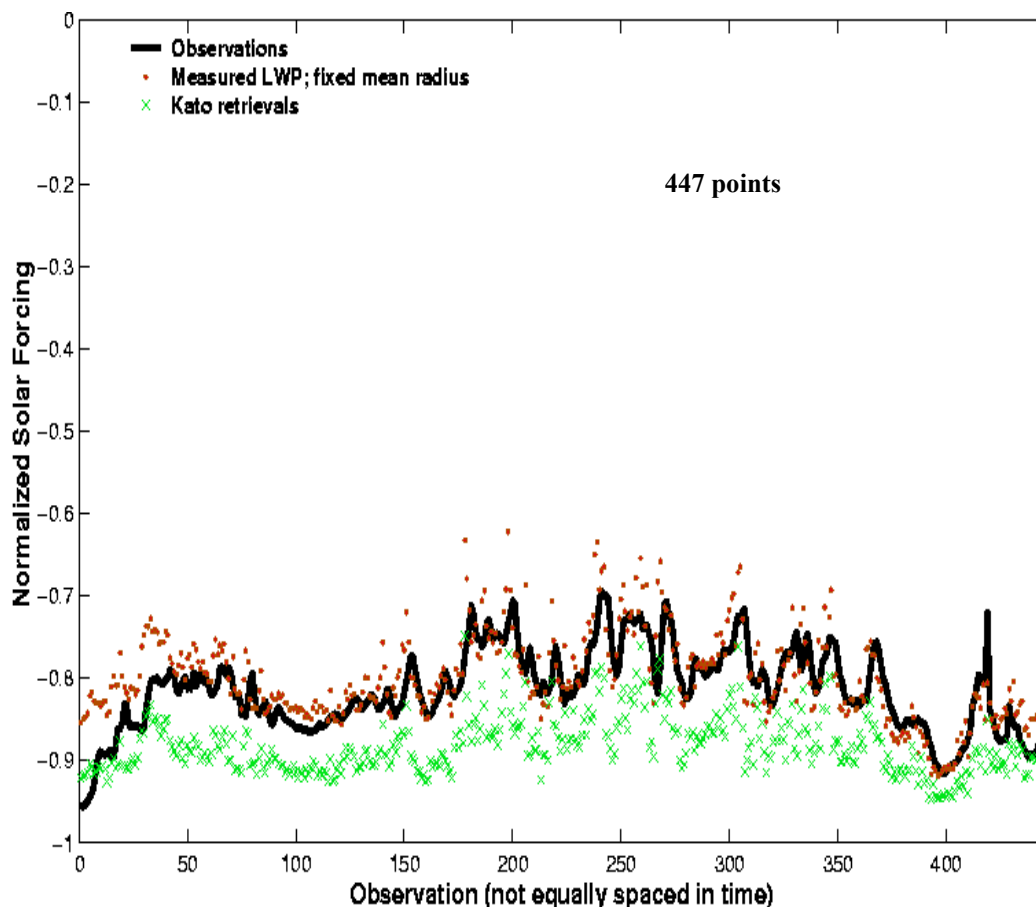


Figure 5b. Time series of normalized forcing (1 minute averaged calculations) for December 3, 1997. The rms error for the climatological radius of $7.5 \mu\text{m}$ is 0.04, while it is $0.077 \mu\text{m}$ for the retrievals.

Therefore, if the regression is constrained so that the 0 of the observations match the 0 of the calculations and retrievals, the regression line closely matches the observations in both the cases (pink dotted lines in Figures 4a and 4b).

The performance of the retrievals should be considered in the context of the performance of the fixed climatological radius. This is better illustrated in Figures 5a and 5b, which show the time series of two days in detail.

The root mean square (rms) error in the two cases, for the climatological radius is 0.051 and 0.04, respectively. Therefore, it is obvious that the climatological radius by itself produces good agreement with the observations. The retrievals perform well in the first case but have a significant bias in the second. The other days (not shown) were also compared individually but none of them showed a better performance when using the retrievals. Also, the median of the control-normalized forcings is -0.66 , which is comparable to that of the observations. On the other hand, the median for the retrievals is -0.7462 . This value is lower than both the observations and the calculations. As we use the same LWP

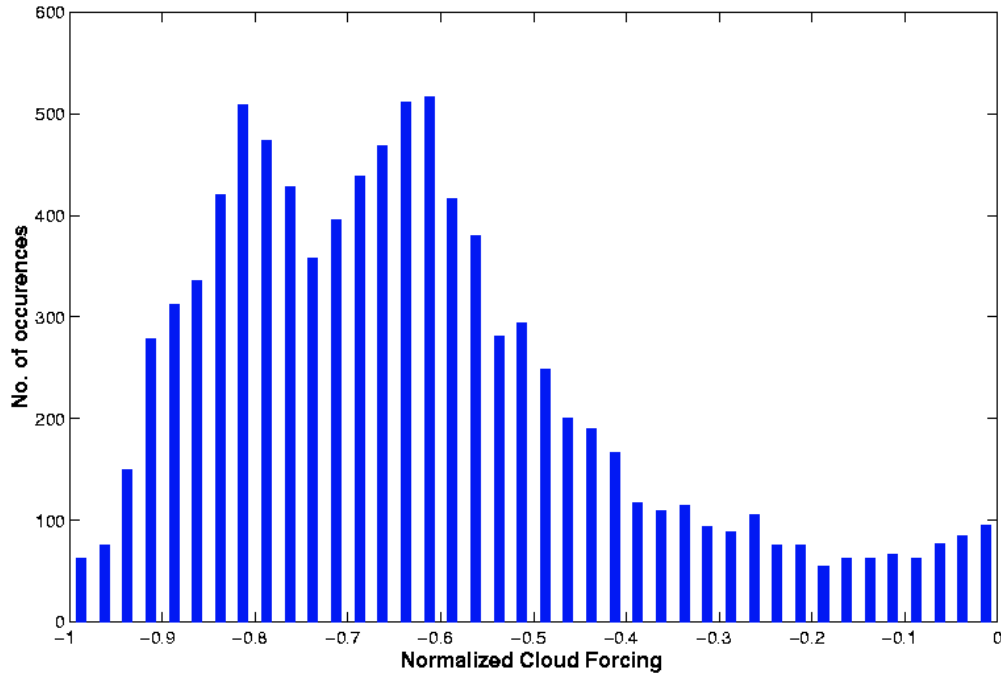


Figure 6. Histogram of the observed normalized cloud forcing divided into bins of size 0.025. The median value of the forcing is 0.65 with predominance of points below -0.4 .

for our calculations, it is clear that on the average, the effective radius for the retrieval are lower than the fixed climatological value. Figure 3 also corroborates this point and shows the mean retrieved radius is $6.57\mu\text{m}$, which is nearly $1\mu\text{m}$ smaller than the climatological value.

Conclusions

Our primary goal was to assess the performance of size retrievals of stratus clouds when compared to climatology. It is interesting to note that usage of a tuned climatological radius leads to results with a high correlation and low rms error. In order to perform better than the climatology the size retrievals have to drive down errors to levels lower than can be done at this stage. Therefore, contrary to what we would expect, the retrievals have a higher scatter than the climatology even though they fit well with the observations. Therefore, the retrievals end up showing no skill when compared to climatology. This leads to two questions. The first concerns the sources of errors in the retrievals and whether they are rectifiable, given our present level of understanding. The second is whether the second order sensitivity of the radius requires a better value of radius and what proportion of the errors is attributable to uncertainties in LWP.

Addressing the first question we can see that the errors may be the effect of propagating errors in either one or both the inputs to the retrievals namely the radar reflectivities and the LWPs from the MWR. It has recently been identified that the radar reflectivities in the near field are biased lower than normal. On the other hand, it has been established that the noise floor of the MWR is 0.03 mm . Additionally, the minimum level of uncertainty in LWP retrievals in the best possible case is 0.01mm . The MWR-derived

LWP can therefore have errors of over 100% in a significant number of cases as the measurements have a median value of 0.07, if we neglect outliers with very high values. These outliers are possibly due to condensation on the instrument. It may also be possible that the drop size distribution is bimodal in reality. This can lead to significant errors in retrievals. The only solution in the case of bimodal distributions is the collection of spectral data using the radar. Currently, the MMCR does not collect spectra on an operational basis but there is an apparent need to do so.

One possible way of reducing the errors in the LWP retrieval is to use an infrared retrieval to get LWPs in cloud with emissivities less than unity. We are currently trying to devise a retrieval that, if successful, will lead to reduction in the uncertainties in LWP.

Corresponding Author

M. Sengupta, manajit@pnl.gov, (509) 375-2504

References

Clothiaux, E. E., T. P. Ackerman, G. G. Mace, K. P. Moran, R. T. Marchand, M. A. Miller, and B. E. Martner, 2000: Objective determination of cloud heights and radar reflectivities using a combination of active remote sensors at the ARM CART Sites. *Appl. Meteor.*, **39**, 645–665.

Considine, G., J. A. Curry, and B. Wielicki, 1997: Modeling cloud fraction and horizontal variability in marine boundary layer clouds. *J. Geophys. Res.*, **102**, 13,517-13,525.

Hansen, J. E., and L. D. Travis, 1974: Light scattering in planetary atmospheres. *Space Sci. Rev.*, **16**, 527-610.

Harrison, L., J. Michalsky, and J. Berndt, 1994: Automated Multi-filter Rotating Shadowband Radiometer: An instrument for optical depth and radiation measurements. *Appl. Opt.*, **22**, 5118-5125.

Hartmann, D. L., M. E. Ockert-Bell, and M. L. Michelsen, 1992: The effect of cloud type on the earth's energy balance. *J. Climate*, 1281-1304.

Kato, S., T. P. Ackerman, E. E. Clothiaux, J. H. Mather, G. G. Mace, M. L. Wesely, F. Murcray, and J. Michalsky, 1997: Uncertainties in modeled and measured clear-sky surface shortwave irradiances. *J. Geophys. Res.*, **102**, 25,881-25,898.

Kato, S., G. G. Mace, E. E. Clothiaux, J. C. Liljegren, and R. T. Austin, 2001: Doppler cloud radar derived drop size distributions in liquid water stratus clouds. *J. Atmos. Sci.* **58**, 19, 2895–2911.

Liljegren, J. C., E. E. Clothiaux, G. G. Mace, S. Kato, and X. Dong 2000: Retrieval of cloud liquid water path. *J. Geophys. Res.*, submitted.

Long, C. N., and Ackerman, T. P., 1999: Estimation of fractional sky cover from broadband SW radiometer measurements. In *Proceedings of the Tenth Atmospheric Radiation Measurement (ARM) Science Team Meeting*, U.S. Department of Energy, Washington, D.C.